

# Regulatory association of long noncoding RNAs and chromatin accessibility facilitates erythroid differentiation

Yunxiao Ren,<sup>1-3</sup> Junwei Zhu,<sup>1,2,4</sup> Yuanyuan Han,<sup>5</sup> Pin Li,<sup>1</sup> Jing Wu,<sup>1,3</sup> Hongzhu Qu,<sup>1,2,4</sup> Zhaojun Zhang,<sup>1-4</sup> and Xiangdong Fang<sup>1,2,4,6</sup>

<sup>1</sup>CAS Key Laboratory of Genome Science & Information, Beijing Institute of Genomics, Chinese Academy of Sciences/China National Center for Bioinformation, Beijing, China;

<sup>2</sup>Institute for Stem Cell and Regeneration, Chinese Academy of Sciences, Beijing, China; <sup>3</sup>Sino-Danish College, University of Chinese Academy of Sciences, Beijing, China;

<sup>4</sup>Beijing Key Laboratory of Genome and Precision Medicine Technologies, Beijing, China; <sup>5</sup>Guizhou University, Medical College, Guiyang, China, China; and <sup>6</sup>University of Chinese Academy of Sciences, Beijing, China

## Key Points

- LncRNAs regulate erythroid differentiation through coordinating with chromatin accessibility.
- The integrative multi-omics analysis reveals stage-specific regulatory association of lncRNAs and chromatin accessibility in erythropoiesis.

Erythroid differentiation is a dynamic process regulated by multiple factors, whereas the interaction between long noncoding RNAs (lncRNAs) and chromatin accessibility and its influence on erythroid differentiation remains unclear. To elucidate this interaction, we used hematopoietic stem cells, multipotent progenitor cells, common myeloid progenitor cells, megakaryocyte-erythroid progenitor cells, and erythroblasts from human cord blood as an erythroid differentiation model to explore the coordinated regulatory functions of lncRNAs and chromatin accessibility by integrating RNA-seq and ATAC-seq data. We revealed that the integrated network of chromatin accessibility and lncRNAs exhibits stage-specific changes throughout the erythroid differentiation process and that the changes at the erythroblast stage of maturation are dramatic. We identified a subset of stage-specific lncRNAs and transcription factors (TFs) that associate with chromatin accessibility during erythroid differentiation, in which lncRNAs are key regulators of terminal erythroid differentiation via an lncRNA-TF-gene network. LncRNA *PCED1B-AS1* was revealed to regulate terminal erythroid differentiation by coordinating GATA1 dynamically binding to the chromatin and interacting with the cytoskeleton network during erythroid differentiation. *DANCR*, another lncRNA that is highly expressed at the megakaryocyte-erythroid progenitor cell stage, was verified to promote erythroid differentiation by compromising megakaryocyte differentiation and coordinating with chromatin accessibility and TFs, such as RUNX1. Overall, our results identify the associated network of lncRNAs and chromatin accessibility in erythropoiesis and provide novel insights into erythroid differentiation and abundant resources for further study.

## Introduction

The human body produces approximately  $2 \times 10^{11}$  erythroid cells per day to meet the requirements for oxygen delivery and carbon dioxide exchange.<sup>1</sup> In adults, the process of erythropoiesis is generated from hematopoietic stem cells (HSCs) in bone marrow, which differentiate into multipotent progenitor (MPP) cells and common myeloid progenitor (CMP) cells, followed by differentiation into megakaryocyte-erythroid progenitor (MEP) cells, erythroid progenitor cells, and erythroblasts (EBs), which then

Submitted 3 May 2021; accepted 13 September 2021; prepublished online on *Blood Advances* First Edition 13 October 2021; final version published online 10 December 2021. DOI 10.1182/bloodadvances.2021005167.

RNA-seq datasets for *DANCR*-overexpressed K562 cells are available in the Genome Sequence Archive (accession number CRA003708) (<https://ngdc.cncb.ac.cn/gsa/s/xCA571e5>).

For other original data, please contact [fangxd@big.ac.cn](mailto:fangxd@big.ac.cn) or [zhangzhaojun@big.ac.cn](mailto:zhangzhaojun@big.ac.cn). The full-text version of this article contains a data supplement.

© 2021 by The American Society of Hematology. Licensed under Creative Commons Attribution-NonCommercial-NoDerivatives 4.0 International (CC BY-NC-ND 4.0), permitting only noncommercial, nonderivative use with attribution. All other rights reserved.

denucleate to form reticulocytes that are released into the bloodstream, where they eventually become erythrocytes.<sup>2</sup>

Erythroid differentiation is a dynamic and precisely regulated process at multiple levels. Any abnormal regulation may damage the formation of erythroid cells, which will cause erythropoiesis-related diseases. Previous studies have made advancements in elucidating the roles of cytokines, transcription factors (TFs), microRNAs, epigenetic modifiers, and signaling pathways,<sup>3-6</sup> but the regulatory mechanisms of the interactivity of long noncoding RNAs (lncRNAs) and chromatin accessibility lack comprehensive exploration during erythroid differentiation.

The chromatin structure is essential for gene expression. Chromatin accessibility enables access to TFs that specify the transcriptional regulation in certain cell type, and this epigenetic variance determines lineage commitment and hematopoietic differentiation process.<sup>7-11</sup> Previous studies defined some characteristics regarding transcriptome and chromatin accessibility during erythroid differentiation and explored the regulatory mechanism of erythropoiesis at multiple omics levels.<sup>10-13</sup> However, few studies have focused on the interaction between lncRNA and chromatin accessibility during erythroid differentiation that will provide a novel mechanism underlying erythropoiesis in a different way.

lncRNAs have a length >200 nt and are noncoding RNAs with a wide range of mechanisms that combine with DNA, RNA, and protein to regulate gene expression and modify chromatin formation.<sup>14,15</sup> Previous studies found that lncRNAs are involved in the regulation of hematopoiesis and erythroid differentiation.<sup>14-17</sup> Similar to chromatin accessibility, lncRNA expression in erythroid differentiation presents strong stage specificity and poor conservation in species.<sup>10,18,19</sup> We infer that lncRNAs could associate with chromatin accessibility during erythroid differentiation, which has not been clarified in this field.

To better understand the regulatory functions of chromatin accessibility and lncRNAs during erythroid differentiation, we performed an integrative analysis of the chromatin accessibility and transcriptome data. We established a comprehensive landscape of chromatin accessibility and the dynamics of lncRNAs during erythroid differentiation. We observed that dynamic interactions between lncRNAs and chromatin accessibility are stage specific throughout the erythroid differentiation process and first computationally identified an lncRNA-TF-gene interactive network that regulates terminal erythroid differentiation. Two lncRNAs, including *DANCR* and *PCED1B-AS1*, were functionally characterized as regulators at specific cell stages in coordination with chromatin accessibility and the TFs during erythroid differentiation. Our findings provide new insights into the dynamic interactive network of lncRNA and chromatin in human erythropoiesis, which may lead to the discovery of biomarkers for preventing or treating erythropoietic or hematopoietic diseases.

## Methods

### Cell models and data availability

We used HSCs, MPP cells, CMP cells, MEP cells, and EBs from human cord blood as a cell model of erythroid differentiation. EBs represent the erythroblastic series of erythropoiesis, including pro-E, baso-E, poly-E, and ortho-E. The different cell stages during erythroid differentiation were defined based on BLUEPRINT

project, and the raw RNA-seq data were obtained from the BLUEPRINT<sup>20</sup> database, which include EGAD00001000907, EGAD00001000911, EGAD00001000915, EGAD00001000919, EGAD0000100939, EGAD00001001140, EGAD00001001156, EGAD00001001169, EGAD00001001177, EGAD00001001186, EGAD00001001492, EGAD00001001515, EGAD00001001538, EGAD00001001550, EGAD00001001561, EGAD00001002316, EGAD00001002358, EGAD00001002363, EGAD00001002433, and EGAD00001002478. The ChIP-seq data were downloaded from the BLUEPRINT Data Coordination Center portal. The ATAC-seq data were derived from the GSE74912 dataset. The members of the ethics committee at Beijing Institute of Genomics, Chinese Academy of Sciences unanimously agreed that the research scheme is scientific and in line with the requirements of ethical principles. The data of the subject were kept confidential. The subject signed the informed consent form and was clearly informed of rights and interests.

### Data preprocessing of RNA-seq data and ATAC-seq

FastQC was used to check the quality of RNA-seq and ATAC-seq raw data. Trimmomatic and TrimGalore were used to remove the adapters and low-quality reads. RNA-seq and ATAC-seq reads were then aligned to the human genome (GRCh37/hg19) using STAR<sup>21</sup> and bowtie2, respectively, with the default parameters. RSEM<sup>22</sup> was then used to quantify the transcripts of RNA-seq data, from which a gene expression matrix and transcriptional expression matrix were constructed. We used picard-tools to mark polymerase chain reaction (PCR) duplicates with the parameter "REMOVE\_DUPLICATES=true" for ATAC-seq data. We then filtered the mitochondrial reads of processed ATAC-seq data using samtools and "grep -v chrM" command. ATAC-seq peaks were finally obtained using callpeak function in MACS2<sup>23</sup> with parameters "-nomodel, -shift 100 and -extsize 200." The phantompeakqualtools package was used to calculate the chain cross-correlation<sup>24</sup> for evaluating the ATAC-seq data quality. Bioconductor package ChIPQC was also used to evaluate the signal distribution of the ATAC-seq.<sup>25</sup>

### Functional enrichment analysis of differentially expressed genes

The raw counts matrix was filtered with rowSums equal to 0, and DESeq2 was used for differential analysis. *P* adjust value <.05 and |log2FoldChange|>1 were used as the threshold. The clusterProfiler R package<sup>26</sup> was used to analyze and visualize functional profiles of gene. We combined the results from molecular function, cellular component, and biological process classes of gene ontology and retained the function terms based on enrichment score and *P* value.

### Weighted gene coexpression network analysis

Weighted gene coexpression network analysis (WGCNA) is performed to analyze gene expression patterns of multiple samples, by which genes with similar expression patterns can be clustered into 1 module, so that the correlation between the module and specific traits can be calculated, which facilitates identification of key regulation factors and elucidates mechanisms of biology development, tumorigenesis, and other diseases.<sup>27</sup> We constructed 14 gene coexpression modules of each lineage during erythroid differentiation using WGCNA R package.

The connectivity of an intramodule network refers to the sum of the correlations among genes in that module. Genes with high connectivity within a module are considered hub genes. Hub genes are usually regulatory factors and thus are located upstream in the regulatory network.<sup>27</sup> We selected the modules that were significantly correlated with each cell type and calculated the intraconnectivity among the modules. The hub genes in each module were then screened according to the threshold of module with a connectivity >0.8.

### Differential peak analysis and peak annotation

We chose DiffBind R package for differential peak based on DESeq2<sup>28</sup> and ChIPseeker R package for peak annotation.<sup>29</sup> We first defined the range of promoter as 1 kb upstream or downstream of the transcription start site. AnnotatePeak function was used to annotate peaks. We obtained the genomic distribution feature of the peaks and lncRNAs (ie, promoter, intron, or exon). We annotated the adjacent genes of peaks and extracted all the genes in the promoter and distal regions as well as the annotated genes and then conducted functional enrichment analysis using the clusterProfiler R package.<sup>26</sup>

### TF motif analysis

Motif enrichment analysis of each stage and the differential peaks was performed using HOMER software. The command module "findmotifsgenome.pl" with the parameter "-len 8,10,12" was used to identify motif sequences with lengths of 8, 10, and 12 bp. The motif files were then filtered based on *P* value <1e-10 threshold. The corresponding TFs of the motif were also filtered according to the threshold of FPKM >5. We identified 65 TF motifs enriched in each cell phase during erythroid differentiation and 43 TFs motif enriched in differential peaks. We then selected some TFs with more stage-specific and plotted them with ggplot2 in R.

### Identification of mRNA and lncRNAs

We extracted mRNAs and lncRNAs based on genome annotation files from ensembl. Clustering analyses of mRNAs and lncRNAs were performed using hclust. We then screened for significant lncRNAs that may regulate erythroid differentiation, which integrated the stage-specific lncRNAs with differentially expressed lncRNAs and the lncRNAs intersecting in the accessible chromatin region. We constructed a diagram of the intersection of the three datasets using UpSet plot with TBtools.

### Establishment of lncRNA-TF-gene regulatory network

We predict regulation factors within 1 kb of the lncRNAs and hub genes combining the ChIP-seq/DNase I-seq/ATAC-seq data of EBs from the Cistrome Data Browser toolkit (<http://dbtoolkit.cistrome.org>) with the previously screened lncRNAs.<sup>30-32</sup> Regulatory factors that corresponded to EBs with regulatory potential (RP) scores >0.5 were retained. RP scores are defined by the binding and expression target analysis algorithm,<sup>33</sup> which is used to evaluate how likely factors regulate interested genes or lncRNAs. Factors with high RP scores represent high potential to regulate the given lncRNAs or genes.<sup>33</sup> We then construct a potential lncRNA-TF-gene regulatory network by integrating the TFs, hub genes, and lncRNAs identified before.

## Results

### Dynamics of chromatin accessibility and transcriptome during erythroid differentiation

The peaks number for chromatin accessibility reflects changes of chromatin state. The average peaks of HSCs, MPP cells, and CMP cells are similar, with >100 000 peaks each, whereas the peaks number for MEP began to gradually decrease and then sharply decreased at EB stage, with an average of only 33 457 peaks (Figure 1A). Chromatin accessibility condenses in terminal erythroid differentiation, and erythroid-specific TFs were active to participate in erythroid differentiation, such as GATA1 and KLF1.<sup>34-38</sup> The dramatically decreased peaks may be related to condensed chromatin and/or TF binding. To verify whether the changes at the transcriptome level correspond with chromatin accessibility, we counted the number of genes and lncRNAs. The number of expressed genes in EBs was significantly lower than that at other differentiation stages (Figure 1B). The decreased number of expressed genes may be related to the process of terminal erythroid differentiation and development. However, the number of lncRNAs in EBs increased significantly compared with numbers in adjacent stages, which is different from the changes in chromatin accessibility and expressed genes (Figure 1C). lncRNAs have been observed to act in various ways, including binding to DNA and RNA, regulating TFs and chromatin structures,<sup>39-41</sup> and regulating terminal erythroid differentiation.<sup>39,42,43</sup> Moreover, the average number of lncRNAs in HSCs is also higher than that of adjacent stages (Figure 1C). Previous studies also showed that lncRNAs hosted in HSCs are involved in the regulation of HSC stemness and differentiation.<sup>19,44</sup>

We further analyzed the significantly differential accessible peaks, expressed genes, and lncRNAs during erythroid differentiation. We found that the numbers of differentially chromatin accessible peaks highly correlated with the numbers of differentially expressed genes between stages (Figure 1D). Moreover, there were more upregulated lncRNAs than downregulated lncRNAs between MEP cells and EBs (supplemental Figure 1), which exhibited the importance of lncRNAs in terminal erythroid differentiation. The genomic distribution of accessible chromatin showed that the proportion of accessible chromatin in promoters began to increase at the MEP stage and significantly increased at the EB stage by >75% (Figure 1E). This finding suggests that a large proportion of accessible chromatin distributed in promoters may promote gene expression between MEP cells and EBs. Taken together, dynamic changes in chromatin accessibility and lncRNAs were observed during erythroid differentiation, and the changes during the differentiation from MEP to EB stage were dramatic.

### Characterization of functions associated with chromatin accessibility and the transcriptome during erythroid differentiation

To understand the biological functions of differential chromatin accessibility, differentially expressed lncRNAs, and genes during erythroid differentiation, we performed functional enrichment analysis. Compared with MEP cells, the enhanced accessible chromatins at the EB stage were enriched in the functions of erythroid differentiation (*P* = 3.18e-6), myeloid differentiation (*P* = 7.31e-7), actin cytoskeleton reorganization (*P* = 1.26e-5), and hemoglobin complex

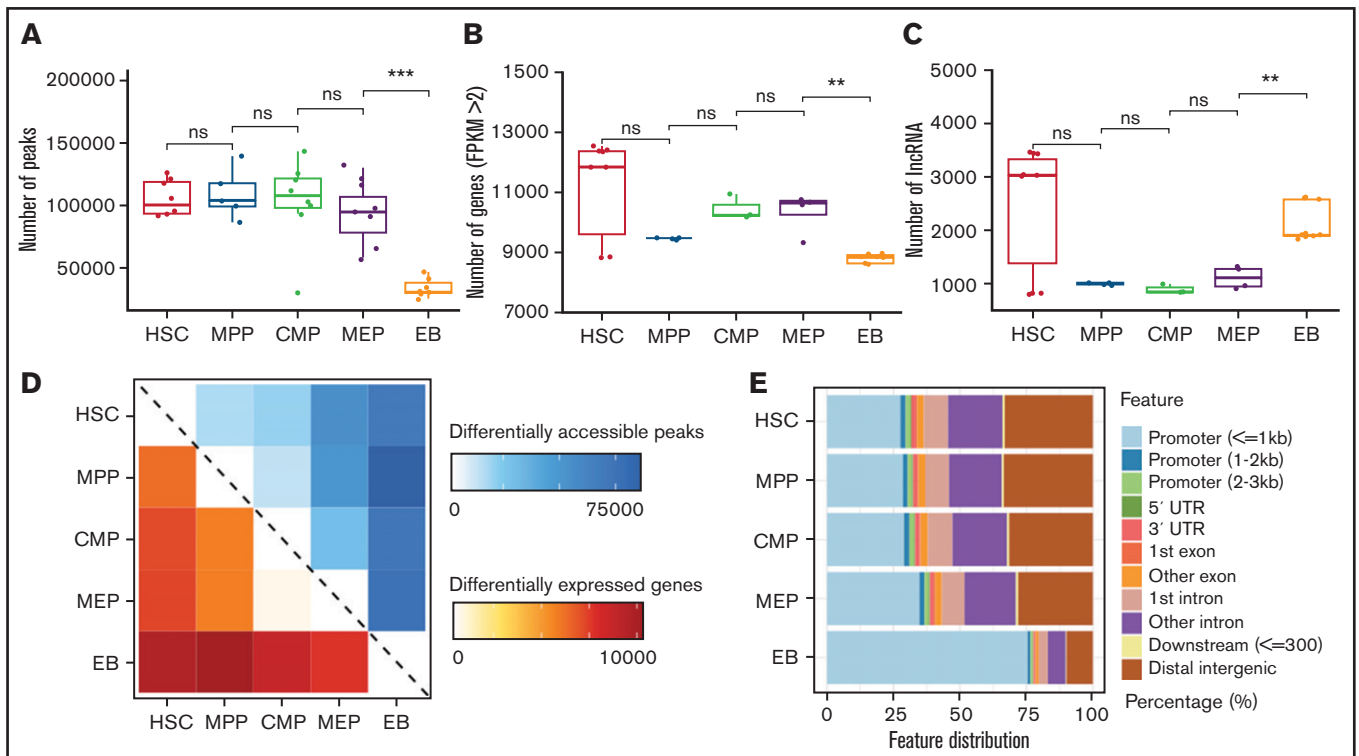


**Figure 1. Dynamic changes in chromatin accessibility and the transcriptome during erythroid differentiation.** (A) Peaks in ATAC-seq data. The boxplot illustrates the number of accessible chromatin regions at each stage during erythroid differentiation. (B) Number of genes at each stage from RNA-seq data with FPKM > 2. (C) Number of lncRNAs at each stage during erythroid differentiation. (D) Heatmap showing the number correlation of differentially accessible peaks of chromatin (top, blue) and differentially expressed genes (bottom, red) during erythroid differentiation. (E) Genomic distribution features of accessible chromatin. The bar plot shows the percentage of ATAC-seq peaks intersecting with the promoter, UTR, exon, intron, and distal intergenic. Statistical results were analyzed using a Kruskal-Wallis test.

( $P = 7.84 \times 10^{-5}$ ) (Figure 2A), which are essential processes during erythroid differentiation.<sup>3</sup> Consistently, the functions of upregulated genes at the EB stage correlated closely with erythroid differentiation, including the functions of tetrapyrrole binding ( $P = 8.02 \times 10^{-6}$ ), heme binding ( $P = 2.95 \times 10^{-5}$ ), hemoglobin complex ( $P = 1.64 \times 10^{-13}$ ), and oxygen transport ( $P = 1.36 \times 10^{-10}$ ) (Figure 2B). Furthermore, we found that higher expression of erythroid-related genes corresponds to more accessible chromatin between MEP cells and EBs (supplemental Figure 2A); however, as control, leukocyte-related genes do not (supplemental Figure 2B).

Interestingly, the enrichment analysis of lncRNAs between MEP cells and EBs showed that only 2 lncRNAs, *LOC107984784* and *LINC01715*, were annotated as relating to the functions of spliceosomal small nuclear ribonucleoprotein complex ( $P = .69 \times 10^{-2}$ ) and pre-mRNA binding ( $P = .67 \times 10^{-3}$ ) (Figure 2C). To explore the relationship between lncRNAs and chromatin, we annotated chromatin accessibility peaks on the lncRNA distribution features and found that peaks related to lncRNA are mainly distributed on distal genomic regions (Figure 2D). In addition to the MEP and EB stage, we also observed the distinct functions underlying the changes in chromatin accessibility and transcriptomes from HSCs to MEP cells (supplemental Figure 2C-D), illustrating that these epigenetic changes represent the stage-specific state during erythroid differentiation.

## Stage-specific TFs and hub genes contribute to erythroid differentiation

Open chromatin can be bound by TFs as an essential process in transcriptional regulation.<sup>45</sup> By integrating chromatin accessibility and the transcriptome profile, we performed motif enrichment analysis and characterized 65 TFs in each stage (Figure 3A; supplemental Table 2) and 44 TFs enriched in differential chromatin accessibility peaks (Figure 3B; supplemental Table 3), demonstrating that the regulation of TFs or chromatin accessibility is cell stage specific during erythroid differentiation. Some TFs are well known to promote erythroid differentiation, such as GATA1 and KLF1,<sup>46,47</sup> whereas the other predicted TFs are also crucial in erythropoiesis, and the underlying mechanism is unclear.

Hub genes refer to highly interconnected nodes in a module that plays significant roles in the regulatory network.<sup>27,48</sup> To further characterize stage-specific hub genes, we clustered genes with similar expression patterns into a module and identified 14 modules (Figure 3C). Each cell stage contains significant coexpression modules (Figure 3D). We selected the modules that were highly related to each stage and identified the hub genes specific to each module. A total of 5 and 12 hub genes were identified in 2 EB modules, the turquoise module and black module, respectively (Figure 3E-F), and 10, 14, 7, and 5 hub genes were identified in the HSC, MPP, CMP,

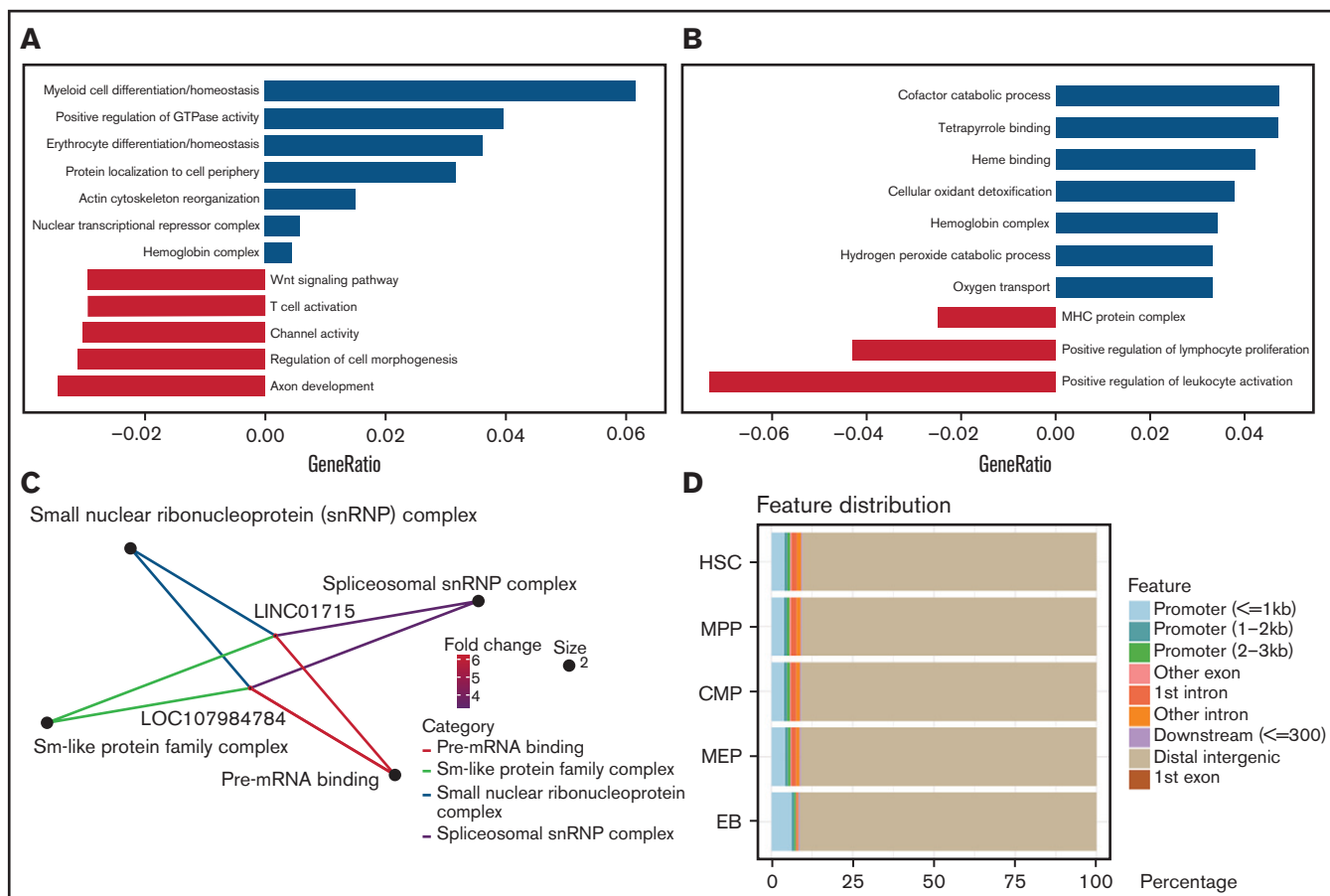


**Figure 2. Function of differentially accessible chromatin and transcriptomes.** (A-C) Functional enrichment of differential chromatin accessibility (A), differentially expressed genes (B), and lncRNAs (C) between the MEP cell and EB stages. (D) Distribution features of chromatin accessibility peaks related to lncRNAs.

and MEP modules, respectively (supplemental Figure 3A-E). *HBG2* and *FECH* were characterized for globin production at EB stage.<sup>49,50</sup> However, more identified hub genes remain to be explored, especially in the turquoise module and black module of EB stage. Taken together, by integrating chromatin accessibility and transcriptome data, we identified stage-specific TFs and hub genes that could be incorporated into interactive networks regulating erythroid differentiation.

### Chromatin-associated lncRNAs are involved in regulatory networks during erythroid differentiation

Hundreds of lncRNAs that promote erythroid differentiation and maturation are expressed specifically at each stage.<sup>42,51</sup> Our clustering results showed that lncRNAs have better cell specificity than mRNA (Figure 4A-B). We extracted stage-specific lncRNAs during erythroid differentiation and displayed the top 10 lncRNAs with specific expression at each stage on a heatmap (Figure 4C). The differential lncRNA analysis showed a larger proportion of downregulated lncRNAs from HSC to CMP (Figure 4D), whereas the proportion of upregulated lncRNAs increased suddenly at the EB stage (Figure 4D), which indicates that lncRNA may play an important role at the late stage of erythroid differentiation.

We next screened lncRNAs that are differentially expressed, located in the differential accessible chromatin region, stage specific, and highly expressed (Figure 4E; supplemental Figure 4 A-C). We identified 4, 3, 2, 1, and 5 lncRNAs at the HSC (supplemental Figure 5 A-E), MPP (supplemental Figure 5 F-G), CMP (supplemental Figure 5 H-I), MEP (Figure 4F), and EB stages, respectively (Figure 4F), that could be associated with erythropoiesis by coordinating accessible chromatin, of which *DANCR* is specifically highly expressed at the MEP stage and was further functionally verified in this study.

### *DANCR* promotes erythroid differentiation by compromising megakaryocyte differentiation

We found that chromatin accessibility and the transcriptome changed dramatically at the MEP stage, which can give rise to megakaryocytes and erythroid cells. *DANCR* was specifically expressed higher at the MEP stage (Figure 4F). *DANCR* is a tumor promoter, but little is known about its function in erythroid differentiation.<sup>52</sup> In this study, we observed that the knockdown of *DANCR* leads to the reduction in the proportion of CD235a<sup>+</sup> erythroid cells (Figure 5A), the production of erythroid progenitors (Figure 5B), and the expression of erythroid-specific genes, including *HBG* and *HBB* (Figure 5C). We also observed the developmental defect of erythroid lineage during erythroid differentiation caused by inhibition of

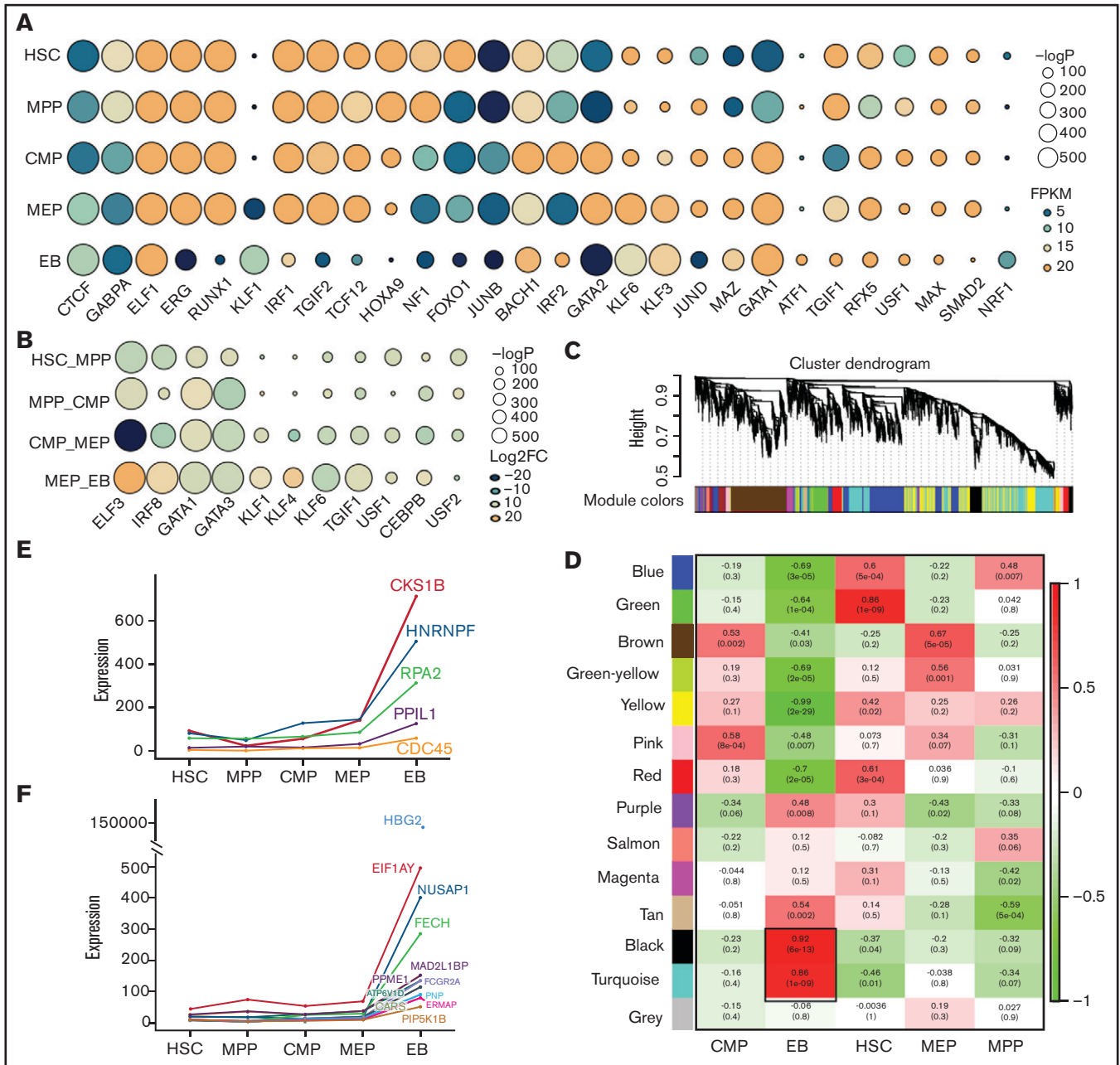
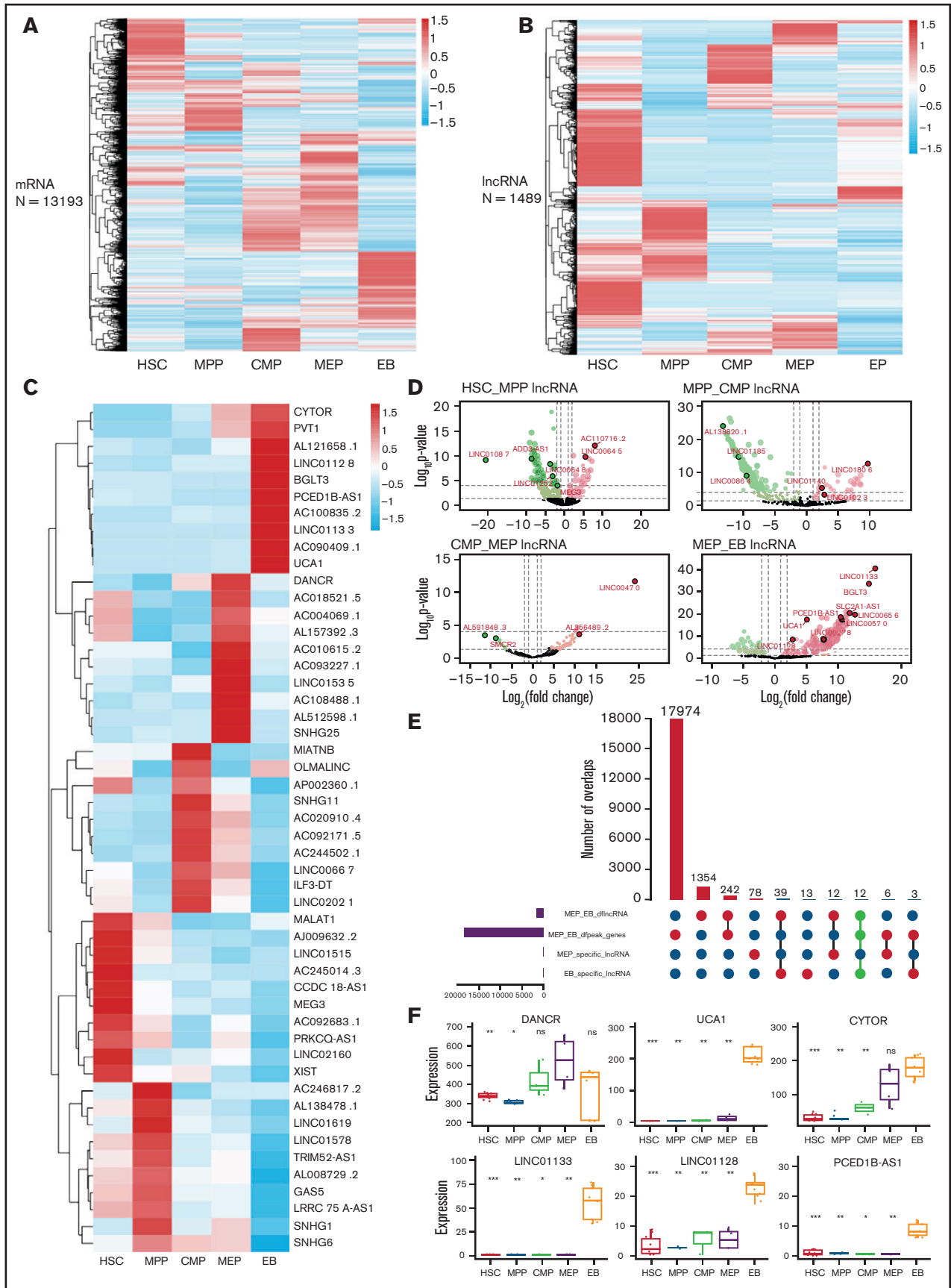


**Figure 3. Transcriptional factors and hub gene identification through chromatin accessibility enrichment analysis and weighted gene coexpression network analysis.** TF motif enrichment of ATAC-seq peaks during erythroid differentiation. (A) TFs specifically enriched at each stage during erythroid differentiation. (B) TFs enriched at differential peaks. (Some of the TFs are shown in the figure according to their enrichment score). The size of the circle represents the  $-\log P$  value, which indicates the significance of TF motif enrichment. The color of circle represents the expression (A, FPKM) and differential fold change (B, log<sub>2</sub>FC) of TFs. (C) Gene cluster dendrogram obtained through linkage hierarchical clustering. The colorful lines below the tree show the modules that were calculated by Dynamic Tree Cutting. (D) The relationships between module and cell type. Each row represents a module eigengene, and each column corresponds to a trait. Each box contains the corresponding correlations and  $P$  value. The colors in the figure are based on the correlations. Expression of hub genes in EB, each shown by its significant module: the turquoise module (E) and the black module (F).

*DANCR* (Figure 5D). We confirmed the phenotypes caused by the overexpression of *DANCR* (supplemental Figure 6A-D). In particular, the overexpression of *DANCR* promotes the expression of globin proteins in differentiated erythroid cells (supplemental Figure 6D). By performing transcriptome sequencing of K562 cells with the

overexpression of *DANCR*, we observed that chromatin-associated functions were disturbed (supplemental Figure 6E), demonstrating that *DANCR* participates in hematopoiesis by coordinating with chromatin. Interestingly, the colony-forming unit assay revealed that overexpression of *DANCR* promotes the production of erythroid



progenitors while inhibiting megakaryotic progenitor cells ( $P < .05$ ) (supplemental Figure 6C). Meanwhile, highly enriched negative regulation of megakaryocyte differentiation was also observed in the transcriptome data of K562 cells (supplemental Figure 6E). These observations could indicate that overexpression of *DANCR* promotes erythroid differentiation by compromising megakaryocyte differentiation. Moreover, we observed strong H3K4me3 and H3K27ac signals around *DANCR* (supplemental Figure 6F), which indicates that this region has enhancer signal.<sup>53</sup>

To further explore the regulatory mechanism of *DANCR* in hematopoiesis, we screened ChIP-seq data<sup>54</sup> and comprehensively identified TFs that appear in the *DANCR* genomic region associated with chromatin accessibility in TF-1 cells (supplemental Table 3). Interestingly, we observed that RUNX1 (Figure 5E), a player in regulating the balance between erythroid and megakaryocytic differentiation through modulating the balance between KLF1 and FLI1,<sup>55</sup> physically binds to accessible chromatin upstream of *DANCR* in TF-1 cells through WashU Browser. These results suggest that *DANCR* may coordinate accessible chromatin to regulate MEP cell differentiation. However, we did not observe the binding of RUNX1 in the corresponding position in the ChIP-seq data of K562 cells in UCSC, which may be the result of TF variability at the chromatin accessibility for specific genes existing in different cell stages and cellular environment between TF-1 and K562 cells.

### Regulatory networks of lncRNAs, TFs, and genes involved in terminal erythroid differentiation

EBs are an important stage of erythroid differentiation involving the expulsion of nucleus, which forms reticulocytes that mature into biconcave red blood cells.<sup>56</sup> The current results indicate that a regulatory network of lncRNAs, TFs, and genes may regulate terminal erythroid differentiation. We therefore integrated ChIP-seq, DNase I-seq, and ATAC-seq data in Toolkit from Cistrome Data Browser to predict the potential regulatory networks at EB stage (Figure 6A).

*PCED1B-AS1* is a novel lncRNA that is specifically expressed at EB stage. Our results showed that knockdown of *PCED1B-AS1* leads to the decrease in the proportion of CD235a<sup>+</sup> cells (Figure 6B) and the expression of erythroid-specific genes compared with control (Figure 6C). Colony formation assay indicated that knockdown of *PCED1B-AS1* results in decreased burst-forming unit-erythroid and colony-forming unit-erythroid colonies (Figure 6D). Morphology analysis showed the developmental delay of erythroid lineage in terminal erythroid differentiation (Figure 6E). The key phenotypes were confirmed with the overexpression of *PCED1B-AS1* (supplemental Figure 7). In particular, the overexpression of *PCED1B-AS1* promotes the expression of globin proteins in differentiated erythroid cells (supplemental Figure 7D). These results demonstrated that *PCED1B-AS1* participates in terminal erythroid differentiation.

Based on the regulatory network constructed, we hypothesize that *PCED1B-AS1* regulates terminal erythroid differentiation cooperating with GATA1. We previously revealed the binding of GATA1 in the genomic regions of *PCED1B-AS1* in K562 cells.<sup>57</sup> In this study, using public ChIP-seq dataset, we screened 4 binding sites of GATA1 in genomic regions of *PCED1B-AS1* in EBs and verified the physical binding of GATA1 in 2 regions (Rank1, Rank4) that gradually increase during erythroid differentiation of CD34<sup>+</sup> cells (Figure 6F-G). The abolishment of the GATA1 binding motif leads to the significantly decreased promoter activity of *PCED1B-AS1* (Figure 6H). These results demonstrated that *PCED1B-AS1* regulates terminal erythroid differentiation coordinating dynamic accessible chromatin or GATA1 binding.

To further explore the underlying mechanism by which *PCED1B-AS1* regulates terminal erythroid differentiation, we conducted the in vitro RNA pull-down assay of *PCED1B-AS1* in cultured EBs. Downregulating GATA1 protein levels is necessary in terminal erythroid differentiation.<sup>58</sup> Interestingly, our pull-down assay demonstrated that GATA1 and its interacting protein USP7 were co-precipitated with *PCED1B-AS1* in EBs (supplemental Table 4). USP7 catalyzes the removal of poly-ubiquitylation chains on GATA1 and stabilizes GATA1, by which it ensures the expression level of GATA1 in the late stage of erythroid differentiation and the participation of GATA1 in the regulation in terminal erythroid differentiation<sup>59</sup> (Figure 6H). This is 1 possible mechanism in which *PCED1B-AS1* participates in terminal erythroid differentiation. Moreover, we observed that a few cytoskeleton and associated proteins, including TUBB, PLEC, ACTN3, and POTEKP, were highly co-precipitated with *PCED1B-AS1*<sup>3,60</sup> (Figure 6H; supplemental Table 5). Because membrane skeleton undergoes dynamic remodeling during terminal erythroid differentiation and chromatin condensation,<sup>3,60</sup> we speculate that *PCED1B-AS1* also could regulate terminal erythroid differentiation by interacting with cytoskeleton network. In all, our study expands the mechanism by which *PCED1B-AS1* participates in terminal erythroid differentiation.

A previous study reported that *UCA1*, whose promoter is occupied by GATA1, functions as a scaffold lncRNA to maintain the stability of *ALAS2* mRNA for heme synthesis,<sup>61</sup> which is one crucial process for globin biosynthesis during erythroid differentiation. Our results expanded the underlying mechanism of *UCA1* to regulate erythroid differentiation by coordinating with more specific TFs, including ATF1, CEBPB, and GABPA, and more potential target genes (Figure 6A). Moreover, the regulatory networks of the other lncRNAs, including *CYTOR*, *LINC01128*, and *LINC01133*, with their TFs and genes were identified for the first time, which need to be further verified for their roles in terminal erythroid differentiation. Taken together, lncRNAs located in the open chromatin region coordinating with TFs participate in erythroid differentiation.

**Figure 4. Identification of potential regulatory lncRNAs by integrating transcriptome and chromatin accessibility during erythroid differentiation.** Clustering results of mRNAs (A) and lncRNAs (B). (C) Top 10 stage-specific lncRNAs expressed during erythroid differentiation. (D) lncRNAs differentially expressed between adjacent stages during erythroid differentiation. (E) The number of intersecting differentially expressed lncRNAs and the accessible chromatin between the MEP cell and EB stage. Bar plot on the left shows the number of differentially expressed lncRNAs and genes between MEP cell and EB and the number of specific lncRNAs in MEP and EB. The dot plot (bottom right) connected by solid lines represents different intersecting points. The bar plot (top right) represents the number of intersections. (F) The expression of lncRNAs with potential regulatory functions at the MEP cell and EB stages. *DANCR* is highly expressed at MEP cell stage. *UCA1*, *CYTOR*, *LINC01133*, *LINC01128*, and *PCED1B-AS1* are highly expressed at EB stage.

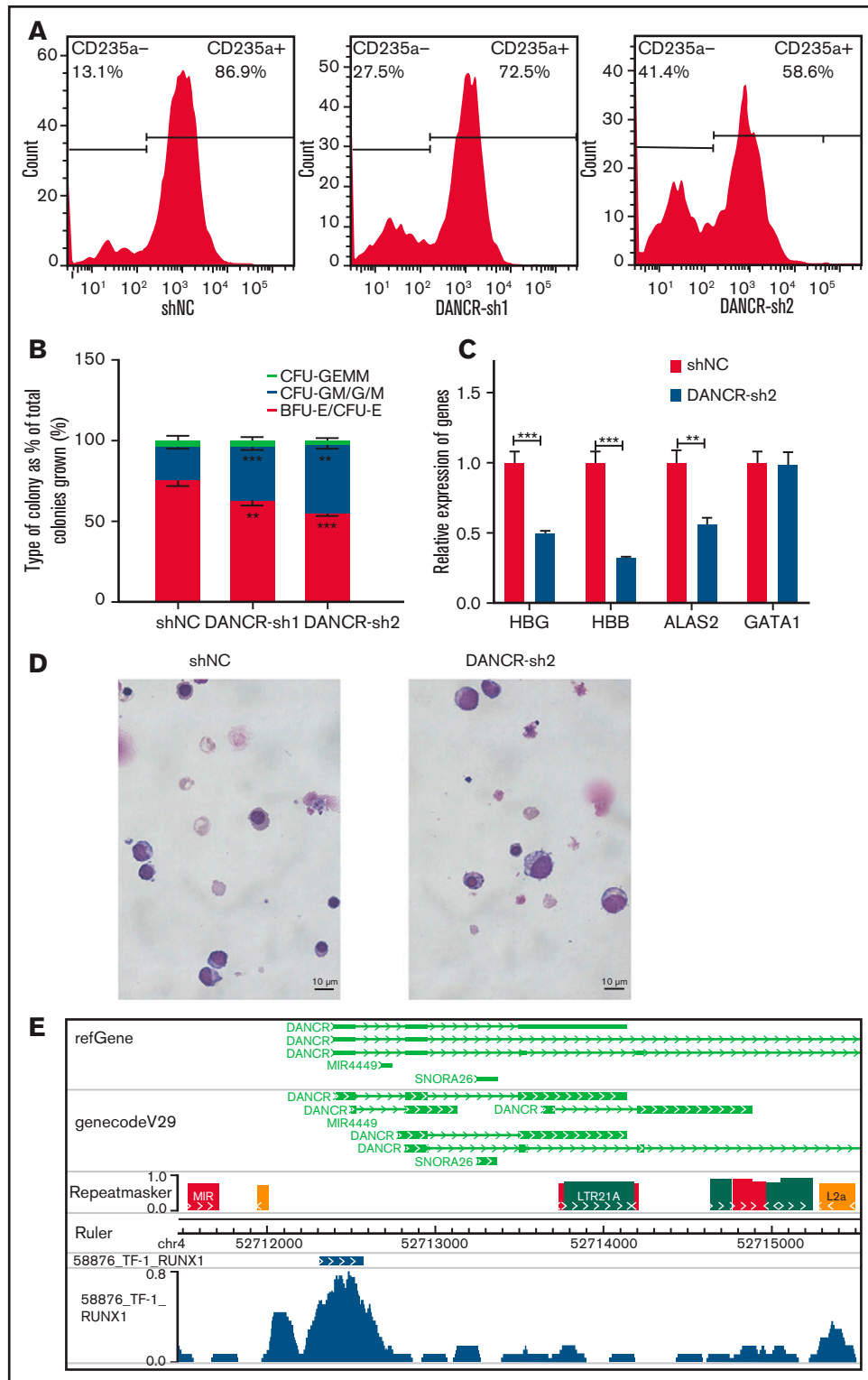


**Figure 5. Aberrant expression of *DANCR* leads to the defects during erythroid differentiation.** (A) The detection of CD235a<sup>+</sup> cells in differentiated CD34<sup>+</sup> cells on day 11 by flow cytometry in green fluorescent protein-positive cells with *DANCR*-KD. The percentage on the right in each figure represents the proportion of CD235a<sup>+</sup> cells. (B) Colony-forming capacity analysis of *DANCR* knockdown in CD34<sup>+</sup> cells. (C) Knockdown of *DANCR* in CD34<sup>+</sup> cells inhibits the accumulation of  $\beta$ -hemoglobin (HBB) and  $\gamma$ -hemoglobin (HBG) proteins and erythroid-specific gene *ALAS2* on Day 12. (D) Morphology in differentiated CD34<sup>+</sup> cells with *DANCR* knockdown and control on Day 11 (original magnification  $\times 100$ ; Wright-Giemsa stain) shows vector control (left) and *DANCR*-KD (right). The size of more differentiated CD34<sup>+</sup> cells with *DANCR* knockdown was larger than that of the control, and the degree of chromatin condensation is reduced. (E) Profile of transcription factor RUNX1 around *DANCR* in TF-1 cells. Statistical results were analyzed by Student *t*-test and Kruskal-Wallis test. \**P* < .05; \*\**P* < .01; \*\*\**P* < .001. Ctrl, control group; KD, knockdown; OE, overexpression.

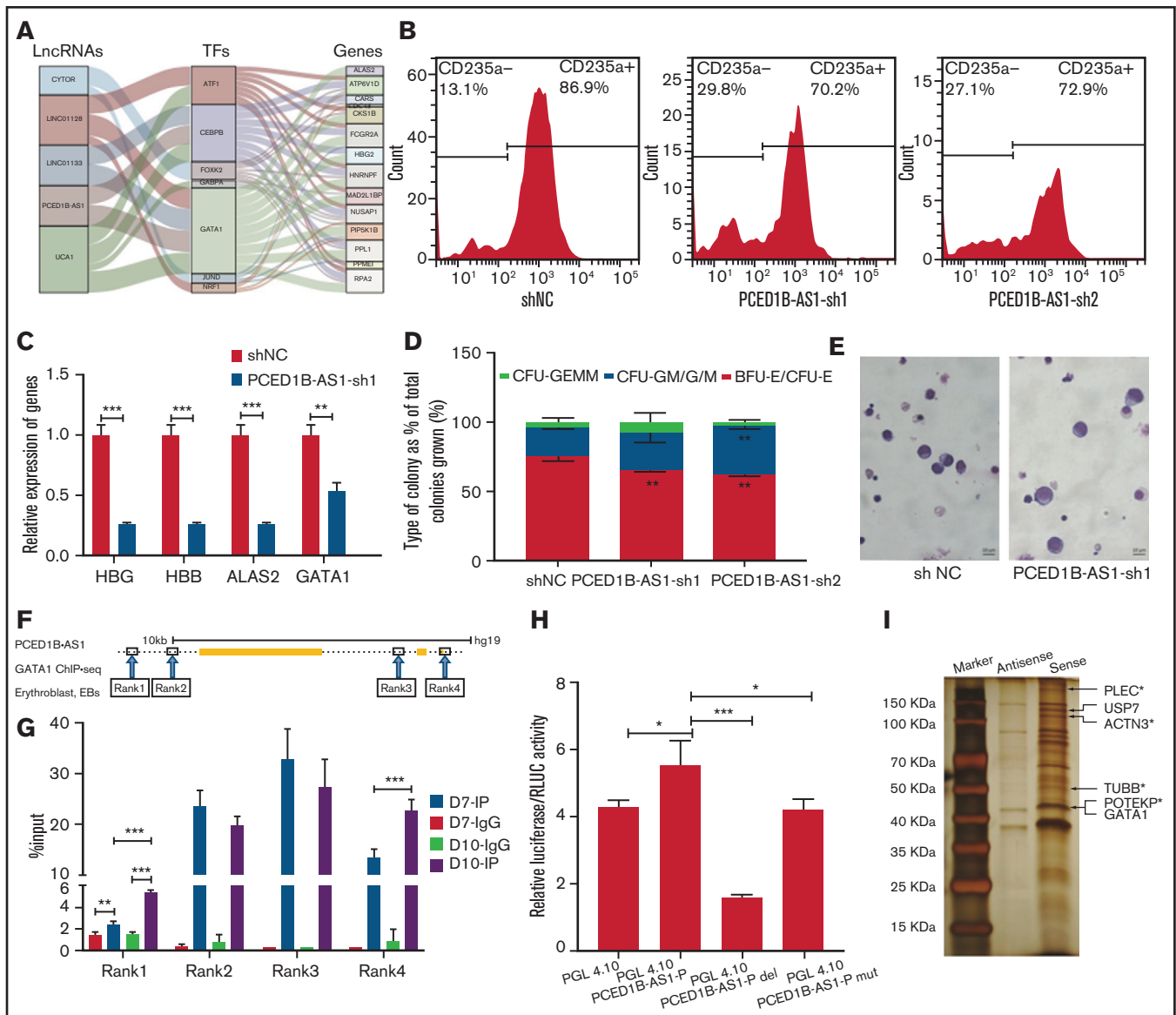


**Figure 6. The regulatory networks of lncRNAs, TFs, and genes during terminal erythroid differentiation.** (A) The lncRNAs-TF-gene regulatory network in EB: specific lncRNA identified in EB (left column); TFs expressed in EB (middle column); and hub genes in EB (right column). The line between the columns represents the possible regulatory relationship among factors. (B) Detection of CD235a<sup>+</sup> cells in differentiated CD34<sup>+</sup> cells on day 11 by flow cytometry in green fluorescent protein-positive cells with *PCED1B-AS1*-KD. The percentage on right in each figure represents the proportion of CD235a<sup>+</sup> cells. (C) Relative expression of erythroid-specific genes in differentiated CD34<sup>+</sup> cells with *PCED1B-AS1*-KD on day 12 detected by qPCR assay. (D) Colony-forming capacity analysis of *PCED1B-AS1* knockdown in CD34<sup>+</sup> cells. (E) Morphology of differentiated CD34<sup>+</sup> cells on day 11 (original magnification  $\times 100$ ; Wright-Giemsa stain): vector control (left) and *PCED1B-AS1*-KD (right). (F) GATA1 binding sites around *PCED1B-AS1* locus in EB stage from ENCODE database (ENCF957CWW). The binding sites are named Rank 1 to 4 from left to right. Rank3 locates in *PCED1B-AS1* locus, and the other 3 binding sites locate outside the *PCED1B-AS1* locus. (G) GATA1 ChIP-qPCR analyses of IgG and IP on Day 7 and Day 10. The GATA1 binding signal was detected at the 4 regions (Rank1, Rank2, Rank3, and Rank4). (H) Detection of activity of *PCED1B-AS1* promoter without any changes or with deletion, mutation on GATA1 binding motif by dual luciferase reporter assay. PGL4.10-*PCED1B-AS1*-P represents the promoter of *PCED1B-AS1* included in the construct of PGL4.10; PGL4.10-*PCED1B-AS1*-P-del represents the deletion of GATA1 binding motif in the promoter; PGL4.10-*PCED1B-AS1*-P-mut represents the mutation of GATA1 binding motif in the promoter. (I) Silver staining of the co-precipitated proteins with lncRNA *PCED1B-AS1* in the in vitro RNA pull-down assay. Cytoskeleton protein or associated proteins indicated by asterisk (\*). Statistical results were analyzed by Student *t*-test and Kruskal-Wallis test; \**P* < .05; \*\**P* < .01; \*\*\**P* < .001. Ctrl, control group; KD, knockdown; OE, overexpression.

## Discussion

In this study, our findings provide a comprehensive landscape of chromatin accessibility, lncRNAs, and hub genes as well as *trans*-factors at each stage during erythroid differentiation and identify the

interactive network of lncRNAs and chromatin accessibility in erythropoiesis, which provides novel insights into erythroid differentiation and abundant resources for further study. We modeled the interactive network of lncRNAs, TFs, and genes in terminal erythroid differentiation and illustrated that several novel lncRNAs are probably

involved in terminal erythroid differentiation cooperating with TFs, which provide new regulatory insights for erythropoiesis.

HSCs and MPP cells are progenitor cells of erythroid differentiation with differentiation ability.<sup>62</sup> Chromatin accessibility tends to decrease from HSCs differentiated into MPP cells as the expressed genes decrease. Some studies have reported that lncRNAs regulate differentiation and proliferation of HSCs, such as *H19* and *MEG3*.<sup>19,63</sup> Interestingly, our results also indicate that downregulated genes in HSCs are associated with noncoding RNA processing. We identified that lncRNA *CCDC18-AS1* was highly expressed in HSCs. Studies showed that *CCDC18-AS1* involved in the cell cycle is similar to *MALAT1*, *NEAT1*, and *H19*.<sup>64</sup> Few studies have been conducted on *LINC01252* and *LINC00648*, which are the other 2 lncRNAs that are highly expressed specific to HSCs. The proportion of enhanced accessible chromatin and upregulated genes is larger during MPP cells differentiated into CMP cells (Figure 1A-B,D), which suggests that transcriptional regulatory activity remains active during MPP cells differentiated into CMP cells and transcriptional regulators can bind to regulate this process.<sup>65,66</sup>

The MEP cell stage involves a continuous transition from CMP cells, in which the cells are bipotent and can further generate 2 completely different functional cells: erythrocytes and platelets. Our results show that chromatin accessibility changes significantly, with greatly decreased accessible chromatin, which indicates that MEP cells prepare to or already possess some characteristics of mature erythroid cells. The functional annotation of changed chromatin accessibility and transcriptome illustrates their association with the functions of myeloid and erythroid differentiation. The differentiation fate of MEPs depends not only on TFs but also on their target genes. Our findings expand the regulation mechanism of MEP differentiation and verify that *DANCR*, which is significantly decreased in KLF1-null neonatal anemia,<sup>67</sup> could promote erythroid differentiation by compromising megakaryocyte differentiation by coordinating TFs. However, the specific target genes that are involved in this process require further verification.

In addition, we identified many novel hub genes and TFs at each stage (Figure 3) that may play important roles during erythroid differentiation, which could facilitate understanding of the molecular networks underlying erythropoiesis. Importantly, we discovered a cluster of known or novel lncRNAs that play significant roles and interact with TFs and genes during erythroid differentiation. It has been reported that *H19* and *MEG3* regulate the differentiation and proliferation of HSCs.<sup>19,63,68</sup> We also identified that *MEG3* is specifically expressed at the HSC stage.

EB is the transition stage between MEP cells and enucleated cells. Chromatin accessibility, lncRNA, and gene expression undergo tremendous changes during the differentiation of MEP cell into EB. Based on the previous study,<sup>57</sup> we further demonstrated that *PCED1B-AS1*, which is significantly decreased in KLF1-null neonatal anemia<sup>67</sup> and human erythroid cell line with sickle cell disease mutation,<sup>69</sup> regulates erythroid differentiation associated with GATA1, chromatin remodeling, and cytoskeleton network in terminal erythroid differentiation. *UCA1* may be involved in erythroid

differentiation by recruiting TFs to target genes and chromatin state changes.<sup>61</sup> Our results identified the interactive network of lncRNAs and chromatin accessibility in erythropoiesis, and the functions of *CYTOR*, *LINC01128*, and *LINC01133* remained to be further elucidated in terminal erythroid differentiation.

It was reported that shRNA knockdown led to off-target inhibition of erythropoiesis.<sup>70</sup> To enhance the specificity of shRNA knockdown *DANCR* or *PCED1B-AS1*, we designed 2 independent shRNAs targeting different regions in *DANCR* or *PCED1B-AS1* and observed consistent phenotypes by different assays. We also confirmed the phenotypes by overexpressing *DANCR* or *PCED1B-AS1*. In addition, it can be further verified by choosing different vectors, better titration, different shRNA controls, and gene editing in the future.

Overall, our study characterized the interactive associated network of lncRNAs and chromatin accessibility during erythroid differentiation by multi-omics integrated analysis. We provide new perspectives and rich resources for exploring the regulatory mechanism underlying erythroid differentiation as well as offer potential markers for preventing or treating various erythropoiesis-related diseases.

## Acknowledgments

This study makes use of data generated by the Blueprint Consortium. A full list of the investigators who contributed to the generation of the data is available at [www.blueprint-epigenome.eu](http://www.blueprint-epigenome.eu). Funding for the project was provided by the European Union's Seventh Framework Program (FP7/2007-2013) under grant agreement no 282510-BLUEPRINT.

This research was supported by grants from the Strategic Priority Research Program of the Chinese Academy of Sciences (XDA16010602), National Natural Science Foundation of China (82070114, 81870097, 81670109, 81700097, and 81700116), and National Key R&D Program of China (2017YFC0907400).

## Authorship

Contribution: X.F. and Z.Z. conceived and supervised the study; Y.R. designed the study and analyzed the data; Z.Z. and H.Q. designed the experiments; J.Z., Y.H., P.L., and J.W. performed the experiments; Y.R. drafted the manuscript; X.F. and Z.Z. revised the manuscript; and all authors read and approved the final manuscript.

Conflict-of-interest disclosure: The authors declare no competing financial interests.

ORCID profiles: Y.R., 0000-0002-0076-0857; J.Z., 0000-0001-9766-3334; Y.H., 0000-0003-1507-0506; J.W., 0000-0001-6032-0979; H.Q., 0000-0001-7013-8409; Z.Z., 0000-0003-0490-6507; X.F., 0000-0002-6628-8620.

Correspondence: Xiangdong Fang, Beijing Institute of Genomics, Chinese Academy of Sciences/China National Center for Bioinformatics, Beijing 100101, China; e-mail: [fangxd@big.ac.cn](mailto:fangxd@big.ac.cn); and Zhaojun Zhang, Beijing Institute of Genomics, Chinese Academy of Sciences/China National Center for Bioinformatics, Beijing 100101, China; e-mail: [zhangzhaojun@big.ac.cn](mailto:zhangzhaojun@big.ac.cn).

## References

1. Vandekerckhove J, Courtois G, Coulon S, Ribeil J-A, Hermine O. Regulation of erythropoiesis. In: EMBT Handbook ([http://www.esh.org/files/doc/IRON2009\\_CAP.2\(44-87\).pdf](http://www.esh.org/files/doc/IRON2009_CAP.2(44-87).pdf)). 2009;44-87.
2. Dzierzak E, Philipsen S. Erythropoiesis: development and differentiation. *Cold Spring Harb Perspect Med*. 2013;3(4):a011601.
3. Nigra AD, Casale CH, Santander VS. Human erythrocytes: cytoskeleton and its origin. *Cell Mol Life Sci*. 2020;77(9):1681-1694.
4. Hattangadi SM, Wong P, Zhang L, Flygare J, Lodish HF. From stem cell to red cell: regulation of erythropoiesis at multiple levels by multiple proteins, RNAs, and chromatin modifications. *Blood*. 2011;118(24):6258-6268.
5. Listowski MA, Heger E, Boguslawska DM, et al. microRNAs: fine tuning of erythropoiesis. *Cell Mol Biol Lett*. 2013;18(1):34-46.
6. Sundaravel S, Steidl U, Wickrema A. Epigenetic modifiers in normal and aberrant erythropoiesis. *Semin Hematol*. 2021;58(1):15-26.
7. Tsompana M, Buck MJ. Chromatin accessibility: a window into the genome. *Epigenetics Chromatin*. 2014;7(1):33.
8. Klemm SL, Shipony Z, Greenleaf WJ. Chromatin accessibility and the regulatory epigenome. *Nat Rev Genet*. 2019;20(4):207-220.
9. Corces MR, Granja JM, Shams S, et al. The chromatin accessibility landscape of primary human cancers. *Science*. 2018;362(6413):1898.
10. Buenrostro JD, Corces MR, Lareau CA, et al. Integrated single-cell analysis maps the continuous regulatory landscape of human hematopoietic differentiation. *Cell*. 2018;173(6):1535-1548.e16.
11. Ludwig LS, Lareau CA, Bao EL, et al. Transcriptional states and chromatin accessibility underlying human erythropoiesis. *Cell Rep*. 2019;27(11):3228-3240.e7.
12. Schulz VP, Yan H, Lezon-Geyda K, et al. A unique epigenomic landscape defines human erythropoiesis. *Cell Rep*. 2019;28(11):2996-3009.e7.
13. Corces MR, Buenrostro JD, Wu B, et al. Lineage-specific and single-cell chromatin accessibility charts human hematopoiesis and leukemia evolution. *Nat Genet*. 2016;48(10):1193-1203.
14. Paralkar VR, Weiss MJ. Long noncoding RNAs in biology and hematopoiesis. *Blood*. 2013;121(24):4842-4846.
15. Satpathy AT, Chang HY. Long noncoding RNA in hematopoiesis and immunity. *Immunity*. 2015;42(5):792-804.
16. Zhang X, Hu W. Long noncoding RNAs in hematopoiesis. *F1000 Res*. 2016;5:1771.
17. Li W, Ren Y, Si Y, Wang F, Yu J. Long non-coding RNAs in hematopoietic regulation. *Cell Regen (Lond)*. 2018;7(2):27-32.
18. Ding N, Xi J, Li Y, et al. Global transcriptome analysis for identification of interactions between coding and noncoding RNAs during human erythroid differentiation. *Front Med*. 2016;10(3):297-310.
19. Zhou J, Xu J, Zhang L, et al. Combined single-cell profiling of lncRNAs and functional screening reveals that H19 is pivotal for embryonic hematopoietic stem cell development. *Cell Stem Cell*. 2019;24(2):285-298.e5.
20. Adams D, Altucci L, Antonarakis SE, et al. BLUEPRINT to decode the epigenetic signature written in blood. *Nat Biotechnol*. 2012;30(3):224-226.
21. Dobin A, Davis CA, Schlesinger F, et al. STAR: ultrafast universal RNA-seq aligner. *Bioinformatics*. 2013;29(1):15-21.
22. Li B, Dewey CN. RSEM: accurate transcript quantification from RNA-seq data with or without a reference genome. *BMC Bioinformatics*. 2014;12:323.
23. Zhang Y, Liu T, Meyer CA, et al. Model-based analysis of ChIP-Seq (MACS). *Genome Biol*. 2008;9(9):R137.
24. Landt SG, Marinov GK, Kundaje A, et al. ChIP-seq guidelines and practices of the ENCODE and modENCODE consortia. *Genome Res*. 2012;22(9):1813-1831.
25. Carroll TS, Liang Z, Salama R, Stark R, de Santiago I. Impact of artefact removal on ChIP quality metrics in ChIP-seq and ChIP-exo data. *Front Genet*. 2014;5:75.
26. Yu G, Wang L-G, Han Y, He Q-Y. clusterProfiler: an R package for comparing biological themes among gene clusters. *OMICS*. 2012;16(5):284-287.
27. Langfelder P, Horvath S. WGCNA: an R package for weighted correlation network analysis. *BMC Bioinformatics*. 2008;9(1):559.
28. Stark R, Brown G. DiffBind: differential binding analysis of ChIP-Seq peak data. <http://bioconductor.org/packages/release/bioc/vignettes/DiffBind/inst/doc/DiffBind.pdf>. Accessed 12 February 2015.
29. Yu G, Wang LG, He QY. ChIPseeker: an R/Bioconductor package for ChIP peak annotation, comparison and visualization. *Bioinformatics*. 2015;31(14):2382-2383.
30. Zheng R, Dong X, Wan C, et al. Cistrome data browser and toolkit: analyzing human and mouse genomic data using compendia of ChIP-seq and chromatin accessibility data. *Quant Biol*. 2020;8(3):267-276.
31. Zheng R, Wan C, Mei S, et al. Cistrome data browser: expanded datasets and new tools for gene regulatory analysis. *Nucleic Acids Res*. 2019;47(D1):D729-D735.
32. Mei S, Qin Q, Wu Q, et al. Cistrome data browser: a data portal for ChIP-Seq and chromatin accessibility data in human and mouse. *Nucleic Acids Res*. 2017;45(D1):D658-D662.
33. Wang S, Sun H, Ma J, et al. Target analysis by integration of transcriptome and ChIP-seq data with BETA. *Nat Protoc*. 2013;8(12):2502-2515.
34. Zhao B, Yang J, Ji P. Chromatin condensation during terminal erythropoiesis. *Nucleus*. 2016;7(5):425-429.

35. Barbarani G, Fugazza C, Strouboulis J, Ronchi AE. The pleiotropic effects of GATA1 and KLF1 in physiological erythropoiesis and in dyserythropoietic disorders. *Front Physiol.* 2019;10:91.
36. Yu X, Martella A, Kolovos P, et al. The dynamic emergence of GATA1 complexes identified in *in vitro* embryonic stem cell differentiation and *in vivo* mouse fetal liver. *Haematologica.* 2020;105(7):1802-1812.
37. Tallack MR, Whittington T, Yuen WS, et al. A global role for KLF1 in erythropoiesis revealed by ChIP-seq in primary erythroid cells. *Genome Res.* 2010;20(8):1052-1063.
38. Villeponteau B, Brawley J, Martinson HG. Nucleosome spacing is compressed in active chromatin domains of chick erythroid cells. *Biochemistry.* 1992;31(5):1554-1563.
39. Sun Q, Hao Q, Prasanth KV. Nuclear long noncoding RNAs: key regulators of gene expression. *Trends Genet.* 2018;34(2):142-157.
40. Luo S, Lu JY, Liu L, et al. Divergent lncRNAs regulate gene expression and lineage differentiation in pluripotent cells. *Cell Stem Cell.* 2016;18(5):637-652.
41. Flynn RA, Chang HY. Long noncoding RNAs in cell-fate programming and reprogramming. *Cell Stem Cell.* 2014;14(6):752-761.
42. Alvarez-Dominguez JR, Hu W, Yuan B, et al. Global discovery of erythroid long noncoding RNAs reveals novel regulators of red cell maturation. *Blood.* 2014;123(4):570-581.
43. Liu J, Li Y, Tong J, et al. Long non-coding RNA-dependent mechanism to regulate heme biosynthesis and erythrocyte development. *Nat Commun.* 2018;9(1):4386.
44. Delás MJ, Jackson BT, Kovacevic T, et al. lncRNA *Spehd* regulates hematopoietic stem and progenitor cells and is required for multilineage differentiation. *Cell Rep.* 2019;27(3):719-729.e6.
45. Gao L, Wu K, Liu Z, et al. Chromatin accessibility landscape in human early embryos and its association with evolution. *Cell.* 2018;173(1):248-259.e15.
46. Ling T, Birger Y, Stankiewicz MJ, et al. Chromatin occupancy and epigenetic analysis reveal new insights into the function of the GATA1 N terminus in erythropoiesis. *Blood.* 2019;134(19):1619-1631.
47. Doré LC, Crispino JD. Transcription factor networks in erythroid cell and megakaryocyte development. *Blood.* 2011;118(2):231-239.
48. Chen L, Yuan L, Qian K, et al. Identification of biomarkers associated with pathological stage and prognosis of clear cell renal cell carcinoma by co-expression network analysis. *Front Physiol.* 2018;9:399.
49. Yan H, Hale J, Jaffray J, et al. Developmental differences between neonatal and adult human erythropoiesis. *Am J Hematol.* 2018;93(4):494-503.
50. Chung J, Wittig JG, Ghamari A, et al. Erythropoietin signaling regulates heme biosynthesis. *eLife.* 2017;6:e24767.
51. Paralkar VR, Mishra T, Luan J, et al. Lineage and species-specific long noncoding RNAs during erythro-megakaryocytic development. *Blood.* 2014;123(12):1927-1937.
52. Jin S-J, Jin M-Z, Xia B-R, Jin W-L. Long non-coding RNA DANCR as an emerging therapeutic target in human cancers. *Front Oncol.* 2019;9:1225.
53. Zhou VW, Goren A, Bernstein BE. Charting histone modifications and the functional organization of mammalian genomes. *Nat Rev Genet.* 2011;12(1):7-18.
54. Li Y, Li X, Yang Y, et al. TRInC: a comprehensive database for human transcriptional regulatory information of lncRNAs. *Briefings in Bioinformatics.* 2021;22(2):1929-1939.
55. Kuvardina ON, Herglotz J, Kolodziej S, et al. RUNX1 represses the erythroid gene expression program during megakaryocytic differentiation. *Blood.* 2015;125(23):3570-3579.
56. Moras M, Lefevre SD, Ostuni MA. From erythroblasts to mature red blood cells: organelle clearance in mammals. *Front Physiol.* 2017;8:1076.
57. Zhu J, Ren Y, Han Y, et al. Long noncoding RNA PCED1B-AS1 promotes erythroid differentiation coordinating with GATA1 and chromatin remodeling. *Blood Science.* 2019;1(2):161-167.
58. Gutiérrez L, Caballero N, Fernández-Calleja L, Karkoulia E, Strouboulis J. Regulation of GATA1 levels in erythropoiesis. *IUBMB Life.* 2020;72(1):89-105.
59. Liang L, Peng Y, Zhang J, et al. Deubiquitylase USP7 regulates human terminal erythroid differentiation by stabilizing GATA1. *Haematologica.* 2019;104(11):2178-2188.
60. Mei Y, Liu Y, Ji P. Understanding terminal erythropoiesis: an update on chromatin condensation, enucleation, and reticulocyte maturation. *Blood Rev.* 2021;46:100740.
61. Gao J, Liu J, Zhang L, et al. Long non-coding RNA-dependent mechanism to regulate heme biosynthesis and erythrocyte development. *Nat Commun.* 2018;9(1):1-15.
62. Eaves CJ. Hematopoietic stem cells: concepts, definitions, and the new reality. *Blood.* 2015;125(17):2605-2613.
63. Mondal T, Subhash S, Vaid R, et al. MEG3 long noncoding RNA regulates the TGF- $\beta$  pathway genes through formation of RNA-DNA triplex structures [published correction appears in *Nat Commun.* 2019;10:5290]. *Nat Commun.* 2015;6(1):7743.
64. Xu J, Shi A, Long Z, et al. Capturing functional long non-coding RNAs through integrating large-scale causal relations from gene perturbation experiments. *EBioMedicine.* 2018;35:369-380.
65. Luo M, Jeong M, Sun D, et al. Long non-coding RNAs control hematopoietic stem cell function. *Cell Stem Cell.* 2015;16(4):426-438.
66. Paul F, Arkin Y, Giladi A, et al. Transcriptional heterogeneity and lineage commitment in myeloid progenitors. *Cell.* 2015;163(7):1663-1677.

67. Magor GW, Tallack MR, Gillinder KR, et al. KLF1-null neonates display hydrops fetalis and a deranged erythroid transcriptome. *Blood*. 2015; 125(15):2405-2417.
68. Sommerkamp P, Renders S, Ladel L, et al. The long non-coding RNA Meg3 is dispensable for hematopoietic stem cells. *Scientific Reports*. 2019; 2110.
69. Demirci S, Gudmundsdottir B, Li Q, et al.  $\beta$ T87Q-globin gene therapy reduces sickle hemoglobin production, allowing for *ex vivo* anti-sickling activity in human erythroid cells. *Mol Ther Methods Clin Dev*. 2020;17:912-921.
70. Traxler EA, Thom CS, Yao Y, Paralkar V, Weiss MJ. Nonspecific inhibition of erythropoiesis by short hairpin RNAs. *Blood*. 2018;131(24):2733-2736.